

Unifying Collisional Models and the Monte Carlo Metropolis Method: Algorithms for Dynamics of Open Quantum Systems

Nathan M. Myers,^{1,*} Hrushikesh Sable,¹ and Vito W. Scarola¹

¹*Department of Physics, Virginia Tech, Blacksburg, VA 24061, USA*

(Dated: March 4, 2024)

Classical systems placed in contact with a thermal bath will inevitably equilibrate to a thermal state at the bath temperature. The same is not generally true for open quantum systems, which place additional conditions on the structure of the bath and system-bath interaction if thermalization is to occur. Collisional models, or repeated interaction schemes, are a category of microscopic open quantum system models that have seen growing use in studying quantum thermalization, in which the bath is modeled as a large ensemble of identical ancilla systems that sequentially interact with the system. We demonstrate that, when each bath ancilla is prepared in a thermal state with a discrete spectrum that matches the energy eigenstate transitions of the system, the system dynamics generated by the collisional model framework are identical to those generated under the Metropolis algorithm. This equivalence holds not just in the steady state regime, but also in the transient regime. As the Metropolis scheme does not require explicitly modeling the system-bath interaction, this allows it to be used as a computationally efficient alternative for simulating collisional model dynamics.

I. INTRODUCTION

The mechanisms and conditions under which a many-body quantum system will thermalize is a question of significant interest that bridges the fields of quantum thermodynamics, condensed matter physics, atomic, molecular, and optical physics, and quantum information. In the context of isolated (closed) quantum systems thermalization of a non-integral many-body quantum system can be achieved under the conditions of the eigenstate thermalization hypothesis [1–4]. However, these conditions are far from guaranteed, and there exists a class of systems that resist thermalization, a phenomena referred to as many-body localization [5, 6].

In the context of open quantum systems it is well established that a quantum system coupled to a heat bath environment evolving under the Markovian Lindblad master equation will equilibrate to a thermal state at the temperature of the bath [7]. While the Lindblad equation is often tractable, it relies on strong assumptions about the dynamics of both the system and environment as well as the system-environment coupling, namely the Born-Markov and rotating wave approximations [7].

In recent years another approach to modeling open quantum systems has seen growing use, especially in the field of quantum thermodynamics, known as collisional models, or repeated interaction schemes [8]. In the collisional model approach the environment is assumed to consist of a collection of many identical subsystems, referred to as ancillae. The interaction between the system and environment occurs as a series of discrete unitary interactions (“collisions”) between the system and one ancilla of the environment. After the interaction, the ancilla is discarded (traced out) and a fresh ancilla is

introduced at the next time step.

By microscopically modeling the system-environment interaction, collisional models have proven particularly useful in studying non-Markovian dynamics (by allowing for correlated ancillae or ancilla-ancilla interactions) [9–14] and non-equilibrium dynamics [15–18]. Notably, the typical Landblad master equation can be derived from the collisional model framework under the assumptions of non-interacting, uncorrelated ancillae [8, 19–21].

The conditions necessary for a collisional model to result in thermalization has seen significant study [22–27]. A critical component for achieving thermalization is the condition that the environment ancillae couple to each transition energy of the system [25]. This is necessary to ensure that the system Hilbert space is fully explored and each energy eigenstate can be populated.

Distinct from the deterministic evolution in the collisional models, the Monte Carlo methods are another class of methods used to study the thermalization of quantum systems [28, 29]. These methods rely upon stochastic sampling of states in the Hilbert space such that the dominant contributions to the ground or the thermal states are captured. These are iterative algorithms wherein each iteration, a random change to the state in the present iteration is considered, thereby generating a trial state. This trial state is either accepted or rejected in the next iteration based on the relative probability of the two states. The trial state is proposed based on some update to the present state only, making this a Markovian process, also referred to as a Markov chain. By stochastic averaging over different chains, the underlying probability distribution can be built. The Markov chain must satisfy the principles of ergodicity and detailed balance to converge to the desired distribution. Here ergodicity implies that every chosen state can be connected to any other state through a finite number of Markov chain moves, to ensure a complete sampling of states. Such Monte Carlo techniques are utilized in understanding the

* myersn1@vt.edu

thermodynamic properties of lattice systems [30, 31] and can also be interpreted as a dynamic process related to the Glauber Kinetic Ising models [32, 33].

Studying open system dynamics has significant practical importance, as very few systems are truly isolated from their environment. Collisional models are conceptually important as they provide a microscopic framework that can operate outside of common assumptions such as weak system-bath interactions. This makes collisional models useful in wide range of contexts including for studying open dynamics in strongly-correlated models [15, 34], quantum optics and simulating light-matter interactions [20, 35], and modeling noise in quantum devices [14]. A notable drawback of the collisional model approach is the need to operate in the joint system-bath Hilbert space, which can become computationally unwieldy, especially for large-dimensional bath ancillae. Here we perform a detailed comparison to show that, subject to certain conditions, when modeling open system thermalization this problem can be circumvented by using a Metropolis Monte Carlo approach that exactly replicates the collisional model dynamics, in both the transient and steady state regimes, without needing to account for the Hilbert space of the bath.

In sections II and III we introduce the collisional model and Metropolis algorithms, respectively, and demonstrate how both approaches can lead to thermalization. In section IV we derive an analytical equivalence between the dynamics produced by both models, and numerically demonstrate the conditions under which this equivalence is achieved using the Heisenberg XXZ chain as a representative model.

II. COLLISIONAL MODEL THERMALIZATION

Following the typical repeated interaction framework we consider a quantum system S and a collection of non-interacting environment ancilla systems a_j . Initially, for a period of t_S the system evolves freely under the dynamics generated by H_S . Then at time t_1 the system interacts with environment ancilla a_1 for time Δt , governed by the interaction Hamiltonian H_{S1} . After the interaction, the environment is traced out, yielding system state $\rho_S(t_1)$,

$$\rho_S(t_1) = \text{tr}_{a_1} \{ U_{S1} [U_S \rho_S(t_0) U_S^\dagger \otimes \rho_{a_1}] U_{S1}^\dagger \} \quad (1)$$

This process, free evolution followed by interaction with a fresh environment ancilla, is then repeated for n time steps. In Fig. 1 we provide a conceptual illustration of the collisional model approach.

Ultimately, we are interested in how this process leads to the thermalization of the system, quantified by whether $\rho_S(t_n)$ approaches a Gibbs state at inverse temperature $\beta = 1/k_B T$,

$$\rho_S(t_n) \rightarrow e^{-\beta H_S} / Z_S. \quad (2)$$

where $Z_S = \text{tr} \{ e^{-\beta H_S} \}$ is the partition function of the system. We begin by assuming that each bath ancilla is

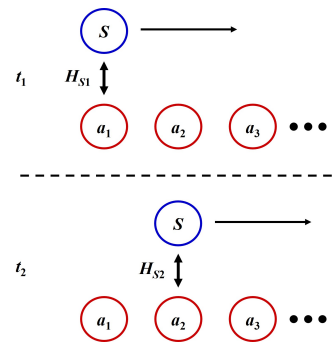


FIG. 1. Illustration of the collision model approach. S represents the system and a_i labels bath ancilla i . The system-bath interaction H_{S1} occurs at time t_1 whereas the interaction H_{S2} occurs at a later time t_2 .

identical and initialized in a thermal state,

$$\rho_a = e^{-\beta H_a} / Z_a \quad (3)$$

Note that, in general, we should not expect the bath thermal state to be the same as that of the system. However, in order to achieve thermalization, the structure of the bath cannot be arbitrary either.

The thermal state is diagonal in the energy eigenbasis, with the population of eigenstate j given by the Boltzmann factor $e^{-\beta E_j} / Z_S$ where E_j is the corresponding eigenenergy. For thermalization of an arbitrary initial state, in order to populate all the energy eigenstates, the system-bath interaction must couple each possible energy eigenstate transition in the system to a corresponding transition in the bath [25]. For microscopically sized baths where the bath spectrum can be well approximated as continuous this condition is trivially satisfied. However, for a bath with a discrete spectrum, as is often the physically relevant case for many-body quantum thermalization, this transition energy matching condition is a crucial consideration.

A. Collisional model thermalization of the XXZ model

As a demonstrative example for how the collisional model can produce thermalization of a many-body quantum system, we consider an N -site one-dimensional XXZ model with open boundaries characterized by the Hamiltonian,

$$H_{XXZ} = -J \sum_{j=1}^{N-1} (\sigma_j^x \sigma_{j+1}^x + \sigma_j^y \sigma_{j+1}^y + \Delta \sigma_j^z \sigma_{j+1}^z) + \frac{h}{2} \sum_{j=1}^N \sigma_j^z \quad (4)$$

where σ^α , $\alpha \in \{x, y, z\}$ are the Pauli matrices. First, let us consider the simple case of $N = 2$. In this case the eigenenergies are,

$$\begin{aligned} E_1 &= -h - J\Delta, & E_2 &= J(\Delta - 2), \\ E_3 &= h - J\Delta, & E_4 &= J(2 + \Delta). \end{aligned} \quad (5)$$

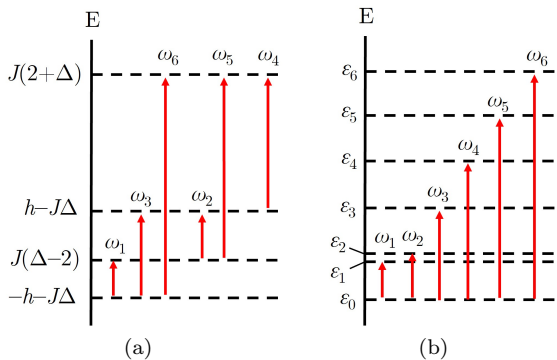


FIG. 2. Diagrams of the (a) system and (b) bath energy spectra for the one-dimensional two-site XXZ model. The red arrows indicate all possible transition energies in the system, and show how those transitions are matched in the bath spectrum.

Let us now consider the structure of the bath. In order to guarantee the energy matching condition for thermalization is fulfilled we assume that the bath consists of an $M + 1$ -level system where M is the total number of transitions between the system's energy eigenstates. The bath's energy levels are spaced such that each transition energy in the system, $E_i - E_j$, corresponds to an energy gap between the bath ground state and a corresponding excited state $|\alpha_{i,j}\rangle$, $\epsilon_{\alpha_{i,j}} - \epsilon_0$. The thermal state of each bath ancilla is thus,

$$\rho_a = \frac{1}{Z_a} \sum_{\alpha_{i,j}=0}^M e^{-\beta \epsilon_{\alpha_{i,j}}} |\alpha_{i,j}\rangle \langle \alpha_{i,j}| \quad (6)$$

where $Z_a = \sum_{\alpha_{i,j}} e^{-\beta \epsilon_{\alpha_{i,j}}}$ is the typical partition function. The bath operators, $B_{\alpha_{i,j}} \equiv |0\rangle \langle \alpha_{i,j}|$ correspond to the jump operator between the ground state of the bath and excited state $|\alpha_{i,j}\rangle$. Similarly, the system operators, $A_{i,j} \equiv |j\rangle \langle i|$ correspond to the jump operator between the system energy eigenstates. Assuming that the system energy eigenvalues are labeled such that $E_1 \leq E_2 \leq E_3 \dots$, the interaction Hamiltonian can be written as,

$$H_I = g \sum_{i>j} (|j\rangle \langle i| \otimes |0\rangle \langle \alpha_{i,j}| + |i\rangle \langle j| \otimes |\alpha_{i,j}\rangle \langle 0|) \quad (7)$$

For the XXZ chain with $N = 2$, there are $M = \binom{2^N}{2} = 6$ possible system energy eigenstate transitions. Thus, in this case, each bath ancilla has a dimension of $\binom{2^N}{2} + 1$. The spectra for both the system and the bath ancillae is plotted in Fig. 2, demonstrating how the bath spectrum fulfills the transition energy matching condition.

The free evolution for the system is generated by the unitary operator,

$$U_S = e^{-iH_{XXZ}t_s} \quad (8)$$

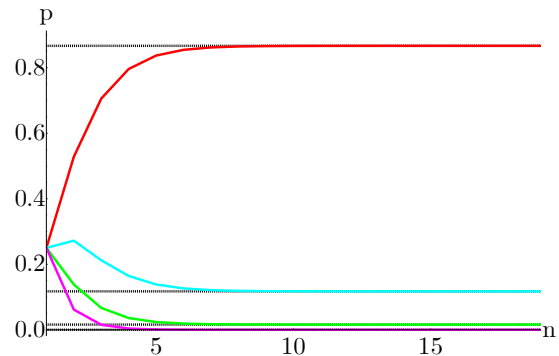


FIG. 3. Occupation probabilities of each energy eigenstate of the two-site XXZ model as a function of the collisional model time step. Dashed horizontal lines indicate the thermal state occupation probabilities for each eigenstate. Parameters are $J = h = \Delta = 1$, $t_s = \Delta t = 1$, $g = 1$, and $\beta = 2$.

while the interaction unitary for each system-ancilla interaction is,

$$U_{Sa} = e^{-iH_I \Delta t}. \quad (9)$$

Combining Eqs. (8), (9), and (6) in Eq. (1), we numerically simulate a 20 time step collisional model for the two-site XXZ chain. We assume the initial system density matrix to be the maximally mixed state. In Fig. 3 we plot the occupation probabilities of each energy eigenstate as a function of the time step, n . We see that the occupation probabilities rapidly approach the thermal state values, indicating thermalization.

To verify that thermalization also occurs at larger system sizes, we repeat our collisional model simulation for chains of length $N = 3$ and $N = 4$. As plotting each eigenstate occupation probability rapidly becomes unwieldy at larger system sizes, we instead use the trace distance as our measure of thermalization. The trace distance is defined as,

$$D(\rho, \sigma) = \frac{1}{2} \text{tr} \left\{ \sqrt{(\rho - \sigma)^\dagger (\rho - \sigma)} \right\} \quad (10)$$

In Fig. 4 we plot the trace distance between the time-dependent density matrix and the system thermal state density matrix as a function of the collisional model time step for the one-dimensional XXZ model. We see that the trace distance approaches zero as n increases, demonstrating that the time-dependent density matrix converges to the thermal state. However, as system size increases, more collisions are required to thermalize the system.

III. THERMALIZATION UNDER THE MONTE CARLO METROPOLIS ALGORITHM

Next, we construct a Monte Carlo algorithm with Metropolis [36] updating to demonstrate thermalization

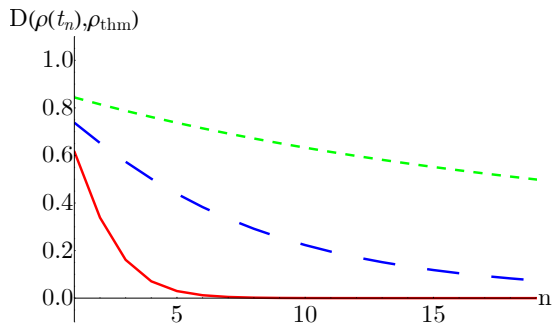


FIG. 4. Trace distance between the time-dependent density matrix and the system thermal state density matrix as a function of the collisional model time step for the one-dimensional XXZ model with $N = 2$ (red, solid), $N = 3$ (blue, dashed), and $N = 4$ (green, dotted). Parameters are $J = h = \Delta = 1$, $t_s = \Delta t = 1$, $g = 1$, and $\beta = 2$.

of the XXZ model in the same context as the collisional model. Our approach is closely related to the Monte-Carlo wave function method [37–39] and the quantum trajectories method [40] used in quantum optics. There are also generalizations of the Metropolis scheme to the quantum regime that exploit circuit-based designs [41].

The Metropolis updating technique [36] was introduced as an algorithm to significantly improve Monte Carlo convergence. The goal of the Metropolis scheme is to generate a sequence of states such that the distribution of these states closely resembles the desired distribution. The key feature of this sampling procedure is using the Metropolis filter function when deciding to accept or reject a proposed move. There are two steps involved in this method. The first one is to propose a move from the present state x to x' , which is based on the conditional proposal probability $G(x'|x)$. The next step involves the acceptance probability $A(x'|x)$ which then determines the acceptance of the proposed move. The detailed balance condition requires, $A(x'|x)G(x'|x)P(x) = A(x|x')G(x|x')P(x')$, where $P(x)$ is the underlying probability distribution to be sampled. Note that the normalization factor in $P(x)$ gets canceled and thus the stochastic averaging can be done without explicitly computing the normalization factor, one key advantage of the Metropolis method. In the context of thermalization, $P(x)$ is the Gibbs distribution, with the partition function as the normalization factor. Thus the accept and reject criteria are based on the energy difference between the proposed and the current state. For classical systems, for instance, spin systems, the updates are often local, involving the flipping of the spin at the chosen site. However, in general, the update scheme can also be non-local [42, 43]. Since the spin basis states are the eigenstates of the classical spin Hamiltonians, these “classical” updates are sufficient to produce thermalization.

In the context of quantum systems, the eigenvectors are, in general, non-trivial superpositions of the spin ba-

sis states. In this case, the classical spin updates are not sufficient to achieve thermalization. To do so, the update scheme must ensure the algorithm explores all the system eigenstates. This can be done using eigenstate jump operators, whose action produces a jump from the present eigenstate to any other eigenstate. The simplest choice for the proposal probability $G(x'|x)$ is a uniform distribution, meaning that all possible “jumps” from the present eigenstate to other eigenstates will be proposed with equal probability. The Markov chain constructed in this way is a sequence of eigenstates weighted by the thermal distribution. Consequently, the low energy states are more probable in the Markov chain in comparison to the high energy states.

For studying thermalization, we consider an update scheme based on the jumps between the different eigenstates. The steps of the algorithm are outlined in Algorithm 1. The first step involves computing the eigenvectors $\{\psi_i\}$ and eigenvalues $\{E_i\}$ of the XXZ Hamiltonian given in Eq. 4 for a system of size N . The set of eigenvectors and eigenvalues can then be used for the Metropolis updating scheme. We consider one eigenstate, ψ_i , chosen randomly from a uniform distribution, and then consider a jump to some other eigenstate ψ_k , also chosen randomly. We then use the Metropolis condition to decide whether the jump from ψ_i to ψ_k is accepted. These steps are then repeated n times, and the corresponding time series of states constitutes one sample, also referred to as a Monte Carlo run. The time-dependent density matrix is then constructed by averaging over many Monte Carlo runs.

This stochastic sampling protocol is different conceptually from the collisional model approach. The microscopic modeling of the interaction and the partial tracing steps in the collisional models is replaced by proposing and then accepting or rejecting the jumps between the eigenstates. In other words, the system and the bath interaction followed by the partial tracing of the bath leads to the mixedness in the system density matrix in the collisional model picture. On other hand, in the Metropolis scheme the thermal density matrix is constructed from averaging over many runs. This has computational advantage, as the numerical steps involves dealing with Hilbert space of the system alone, while the same is not true in the collisional models. In the later approach, the combined system and the bath evolves under the interaction Hamiltonian, as mentioned in Eq. 1, thereby involving the computation over the combined Hilbert space.

As an example, the thermalization of the XXZ model using the Metropolis technique is illustrated in Fig. 5. The parameters in the Hamiltonian are: $J = 1, h = 1, \Delta = 1$ and $\beta = 2$. As shown, the probabilities of the evolving state quickly approach the expected thermal probability values based on the thermal density matrix at the chosen inverse temperature.

Algorithm 1: Thermalization using Metropolis Algorithm

Input: System size N , Hamiltonian parameters h_1, h_2, \dots , Inverse temperature β
Input: Number of thermalization steps $num_thermalization$, Number of Monte Carlo runs num_runs .

Function Exact diag(h_1, h_2, \dots):

 .
 return $\{\psi\}, \{E\}$;

Function Metropolis:

 Exact diag(h_1, h_2, \dots);

Data: Initial eigenstate ψ_{ini}

 for $i \leftarrow 1$ to num_runs do

 Initialize system into some randomly chosen eigenstate ψ_{ini} ;

 for $n \leftarrow 1$ to $num_thermalization$ do

 Propose a jump to a new eigenstate ψ' ;

 Calculate the energy of state ψ as $E = \langle \psi | H | \psi \rangle$, and similar for state ψ' . Compute the energy difference

 $\Delta E = E' - E$. Calculate the acceptance ratio $\alpha = \min(1, \exp(-\beta \Delta E))$;

 Generate a random number u from a uniform distribution $[0, 1]$;

 if $u < \alpha$ then

 Accept the proposed eigenstate jump: $\psi \leftarrow \psi'$;

else

 Reject the proposed eigenstate jump: ψ remains unchanged;

 Record the current state ψ .

 Calculate the thermal averages or occupation probabilities of the eigenstates by averaging over Monte Carlo runs.

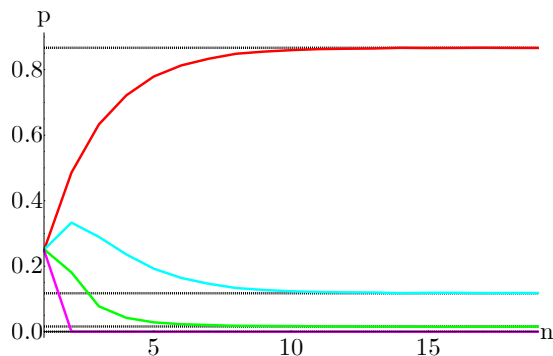


FIG. 5. Occupation probabilities of each energy eigenstate of the two-site XXZ model as a function of the Metropolis algorithm time step, averaged over 100,000 runs. Horizontal black dotted lines indicate the thermal state occupation probabilities for each eigenstate. Parameters are $J = h = \Delta = 1$ and $\beta = 2$.

IV. EQUIVALENCE OF BOTH MODELS

In the previous two sections, we demonstrated that both the collisional model and Metropolis algorithm can result in thermalization. We note that, qualitatively, the evolution of the occupation probabilities appear very similar in both cases, as can be seen by comparing Figs. 3 and 5. In this section we prove explicitly that, under certain conditions, the dynamics generated by both models are identical by showing that the density matrices produced by each individual time step are identical.

A. Collisional model: Single time step evolution

Let us first consider a single time step of the collisional model. The density operator after the interaction with the bath ancilla is given by,

$$\rho_S(t_{n+1}) = \text{tr}_a \{ U_I(t_{n+1}, t_n) [\rho_S(t_n) \otimes \rho_a] U_I^\dagger(t_{n+1}, t_n) \}. \quad (11)$$

We note that in this equation we have not explicitly included the system evolution operators as in Eq. (1). For the purposes of comparing the repeated interaction and Metropolis schemes we are only concerned with the dynamics generated during the system-environment interactions and thus any system evolution that occurs before a collision can be folded into the definition of $\rho_S(t_n)$.

The interaction unitary in Eq. (11) can be expanded iteratively using the Dyson series,

$$U_I(t_{n+1}, t_n) = I - i \int_{t_n}^{t_{n+1}} ds H_I(s) U_I(s, t_n) \quad (12)$$

Taking the limit that the interaction time becomes very short, we can truncate the Dyson series at the second order,

$$U_I(t_{n+1}, t_n) \approx I - i\Delta t H_I - \frac{1}{2} \Delta t^2 H_I^2 \quad (13)$$

where we have assumed that $H_I(t) = H_I$ is time independent and $\Delta t \equiv t_{n+1} - t_n$. Using this expression for

the time evolution operator in Eq. (11) we have,

$$\begin{aligned} \rho_S(t_{n+1}) = & \text{tr}_a \left\{ \rho_S(t_n) \otimes \rho_a + i\Delta t \rho_S(t_n) \otimes \rho_a H_I \right. \\ & - i\Delta t H_I \rho_S(t_n) \otimes \rho_a - \frac{(\Delta t)^2}{2} H_I^2 \rho_S(t_n) \otimes \rho_a \\ & - \frac{(\Delta t)^2}{2} \rho_S(t_n) \otimes \rho_a H_I^2 + (\Delta t)^2 H_I \rho_S(t_n) \otimes \rho_a H_I \\ & - \frac{i(\Delta t)^3}{2} H_I^2 \rho_S(t_n) \otimes \rho_a H_I + \frac{i(\Delta t)^3}{2} H_I \rho_S(t_n) \otimes \rho_a H_I^2 \\ & \left. + \frac{(\Delta t)^4}{2} H_I^2 \rho_S(t_n) \otimes \rho_a H_I^2 \right\}. \end{aligned} \quad (14)$$

The interaction Hamiltonian can be expressed in the general form,

$$H_I = g \sum_{\alpha} (A_{\alpha} \otimes B_{\alpha}^{\dagger} + A_{\alpha}^{\dagger} \otimes B_{\alpha}) \quad (15)$$

where A_{α} and B_{α} are operators in the Hilbert spaces of the system and bath, respectively. Under the assumption that $g\Delta t \ll 1$ we truncate Eq. (14) at the second order in Δt . We further note that any terms in Eq. (14) containing an odd power of H_I will vanish. This is due to the fact that odd number bath correlation functions such as $\text{tr}\{B_{\alpha}\rho_a\}$ and $\text{tr}\{B_{\alpha}^{\dagger}\rho_a\}$ are zero. Thus we can simplify Eq. (14) to,

$$\begin{aligned} \rho_S(t_{n+1}) = & \rho_S(t_n) + \Delta t^2 \text{tr}_a \left\{ H_I \rho_S(t_n) \otimes \rho_a H_I \right. \\ & \left. - \frac{1}{2} H_I^2 \rho_S(t_n) \otimes \rho_a - \frac{1}{2} \rho_S(t_n) \otimes \rho_a H_I^2 \right\}. \end{aligned} \quad (16)$$

We next assume that the bath ancillae are all prepared in identical thermal states structured so that their spectra fulfill the transition energy matching condition, as described in section II. Plugging the interaction Hamiltonian from Eq. (7) and the bath density matrix from Eq. (6) into Eq. (16) and carrying out the partial trace yields,

$$\begin{aligned} \rho_S(t_{n+1}) = & \rho_S(t_n) + \frac{(g\Delta t)^2}{Z_a} \sum_{i>j} \left[A_{i,j} \rho_S(t_n) A_{i,j}^{\dagger} e^{-\beta\epsilon_0} \right. \\ & + A_{i,j}^{\dagger} \rho_S(t_n) A_{i,j} e^{-\beta\epsilon_{\alpha_{i,j}}} - \frac{e^{-\beta\epsilon_0}}{2} \left\{ \rho_S(t_n), |i\rangle \langle i| \right\} \\ & \left. - \frac{e^{-\beta\epsilon_{\alpha_{i,j}}}}{2} \left\{ \rho_S(t_n), |j\rangle \langle j| \right\} \right], \end{aligned} \quad (17)$$

where $\{A, B\} \equiv AB + BA$ is the standard anticommutator.

We pause for a moment here to review the assumptions we have made so far. Equation (17) provides a discrete master equation for the time evolution of the system density matrix generated by a single, very short duration interaction with a thermal bath ancilla. Furthermore, the spectrum of the bath ancilla is engineered

such that there exists an energy gap between the ground state and an excited state of the bath for every possible energy eigenstate transition of the system.

In order to compare directly with the dynamics generated by the Metropolis algorithm, as detailed in the next section, we must make one additional assumption about the system density matrix, $\rho_S(t_n)$. As discussed in Section III the Metropolis algorithm constructs a Markov chain of transitions between the system's energy eigenstates. Thus, the density matrix at any given time step of the algorithm will be a weighted average of the energy eigenstates. For an even comparison, we therefore assume that the system density matrix in the collisional model is also diagonal in the energy eigenbasis, $\rho_S(t_n) = \sum_l p_l(t_n) |l\rangle \langle l|$.

Plugging in this decomposition for the density matrix, Eq. (17) simplifies to,

$$\begin{aligned} \rho_S(t_{n+1}) = & \rho_S(t_n) + \frac{(g\Delta t)^2}{Z_a} \sum_{i>j} \left[\left(A_{i,j} \rho_S(t_n) A_{i,j}^{\dagger} \right. \right. \\ & \left. \left. - p_i(t_n) |i\rangle \langle i| \right) + \left(A_{i,j}^{\dagger} \rho_S(t_n) A_{i,j} - p_j(t_n) |j\rangle \langle j| \right) e^{-\beta\epsilon_{\alpha_{i,j}}} \right] \end{aligned} \quad (18)$$

Where, without loss of generality, we have also set the ground state energy of the bath at zero $\epsilon_0 = 0$.

B. Metropolis algorithm: Single time step evolution

Now let us consider the same situation, namely how the average system state evolves under a single time step of the Metropolis algorithm. For a system with d eigenstates, and thus $L = d-1$ possible transitions between an occupied energy eigenstate to another unoccupied eigenstate, the average system state after a transition is given by,

$$\frac{1}{L} \sum_{i \neq j} \left[A_{i,j} \rho_S(t_n) A_{i,j}^{\dagger} \right] \quad (19)$$

where, as in the case of the collisional model, $A_{i,j} = |j\rangle \langle i|$ is the transition operator between system energy eigenstates $|i\rangle$ and $|j\rangle$. Under the Metropolis algorithm, a transition is accepted with probability $e^{-\beta\omega_{i,j}}$ where $\omega_{i,j}$ is defined as,

$$\omega_{i,j} = \begin{cases} 0 & E_j - E_i < 0 \\ E_j - E_i & E_j - E_i > 0 \end{cases} \quad (20)$$

Accounting for the accept and reject possibilities, the average system state after a single time step is,

$$\begin{aligned} \rho_S(t_{n+1}) = & \frac{1}{L} \sum_{i \neq j} \left[A_{i,j} \rho_S(t_n) A_{i,j}^{\dagger} e^{-\beta\omega_{i,j}} \right. \\ & \left. + (1 - e^{-\beta\omega_{i,j}}) P_i \rho_S(t_n) P_i \right] \end{aligned} \quad (21)$$

Note that the projectors $P_i \equiv |i\rangle\langle i|$ in the second term of Eq. (21) are necessary in order to ensure that the rejection probability $1 - e^{-\beta\omega_{i,j}}$ for the jump $|i\rangle \rightarrow |j\rangle$ only contributes to the summation when $\rho_S(t_n)$ has some population in eigenstate $|i\rangle$. Equation (21) simplifies to,

$$\rho_S(t_{n+1}) = \rho_S(t_n) + \frac{1}{L} \sum_{i \neq j} \left[\left(A_{i,j} \rho_S(t_n) A_{i,j}^\dagger - P_i \rho_S(t_n) P_i \right) e^{-\beta\omega_{i,j}} \right] \quad (22)$$

In order to account for the piece-wise structure of $\omega_{i,j}$ we separate the double summation into terms where $i < j$ and $i > j$,

$$\begin{aligned} \rho_S(t_{n+1}) = \rho_S(t_n) + \frac{1}{L} \sum_{i > j} \left[\left(A_{i,j} \rho_S(t_n) A_{i,j}^\dagger - P_i \rho_S(t_n) P_i \right) \right] \\ + \frac{1}{L} \sum_{i < j} \left[\left(A_{i,j} \rho_S(t_n) A_{i,j}^\dagger - P_i \rho_S(t_n) P_i \right) e^{-\beta(E_j - E_i)} \right] \end{aligned} \quad (23)$$

Noting that $A_{i,j} = A_{j,i}^\dagger$ we can swap the indicies in the second summation of Eq. (23) rewrite it as a single summation,

$$\begin{aligned} \rho_S(t_{n+1}) = \rho_S(t_n) + \frac{1}{L} \sum_{i > j} \left[\left(A_{i,j} \rho_S(t_n) A_{i,j}^\dagger - P_i \rho_S(t_n) P_i \right) \right. \\ \left. + \left(A_{i,j}^\dagger \rho_S(t_n) A_{i,j} - P_j \rho_S(t_n) P_j \right) e^{-\beta(E_i - E_j)} \right] \end{aligned} \quad (24)$$

Under the Metropolis scheme, each experimental run consists of a time series of eigenstates. The density matrix at a particular time step, $\rho_S(t_n)$ is then constructed by averaging over many experimental runs. With this in mind, we can in general represent the density matrix as a weighted average of the system eigenstates,

$$\rho_S(t_n) = \sum_l p_l(t_n) |E_l\rangle\langle E_l|. \quad (25)$$

Plugging Eq. (25) into Eq. (24) yields,

$$\begin{aligned} \rho_S(t_{n+1}) = \rho_S(t_n) + \frac{1}{L} \sum_{i > j} \left[\left(A_{i,j} \rho_S(t_n) A_{i,j}^\dagger - p_i(t_n) |i\rangle\langle i| \right) \right. \\ \left. + \left(A_{i,j}^\dagger \rho_S(t_n) A_{i,j} - p_j(t_n) |j\rangle\langle j| \right) e^{-\beta(E_i - E_j)} \right] \end{aligned} \quad (26)$$

Recalling that, in the collisional model, we structured the bath energies such that $E_i - E_j = \epsilon_{\alpha_{i,j}}$ we can compare Eqs. (26) and (18) and see that they are identical when the condition $1/L = (g\Delta t)^2/Z_a$ is satisfied.

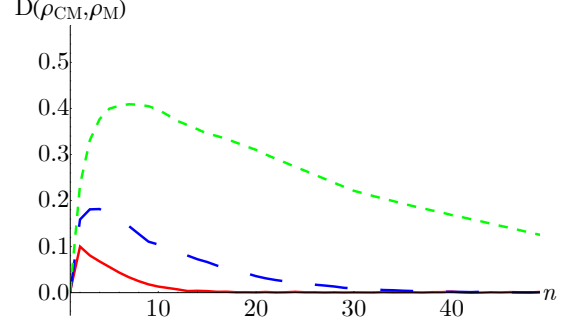


FIG. 6. Trace distance between the density matrix arising from the collisional model and the density matrix arising from the Metropolis algorithm as a function of model time steps, n , for a one-dimensional XXZ chain of length $N = 2$ (red, solid), $N = 3$ (blue, long dashed), and $N = 4$ (green, short dashed). Parameters are $J = h = \Delta = 1$ and $\beta = 2$. For the collisional model we have fixed the interaction parameter $g\Delta t = \sqrt{Z_a/L}$ and for the Metropolis algorithm we have constructed the density matrix from averaging over 100,000 runs.

C. Conditions of equivalence

In this subsection we will consider in detail the conditions necessary to fulfill the equivalence demonstrated in the previous two subsections. Analytically, we have shown that the discrete time evolution of the density matrix generated by the collisional model, Eq. (18), and the Metropolis algorithm, Eq. (26) have exactly the same structure. However, we note that the truncated expansion in Eq. (16) used to derive the time-evolved collisional model density matrix is only accurate under the condition that $g\Delta t \ll 1$. Furthermore, the collisional model bath ancillae must be structured in a thermal state that fulfills the transition energy matching condition. Finally, as noted previously, the exact equivalence between Eqs. (26) and (18) requires $1/L = (g\Delta t)^2/Z_a$.

To compare the validity of this equivalence, in Fig. 6 we plot the trace distance between the density matrix generated by Eq. (11) for the collisional model and the density matrix arising from averaging over 100,000 runs of the Metropolis scheme for the one-dimensional XXZ model. Specifically, we use Eq. (11) for the collisional model, rather than Eq. (18), as we wish to test the regimes in which the approximations that went into the derivation of Eq. (18) are valid. We see that the trace distance initially increases, before dropping back to zero, as both models ultimately result in the thermal state density matrix. We also see that the amount by which the trace distance increases depends on the system size, with shorter length chains having a significantly lower maximum trace distance.

In our comparison, we have fixed the collisional model interaction parameter using the condition $(g\Delta t)^2 = Z_a/L$. Thus, the only source of the deviation between the density matrices for both models comes from the fact

that the truncated expansion of the time evolution operator does not fully capture the dynamics of the collisional model. In order to satisfy both the conditions $g\Delta t \ll 1$ as well as $1/L = (g\Delta t)^2/Z_a$ we see that we want the ratio of Z_a/L to be as small as possible. In Fig. 7 we plot this ratio as a function of chain length for different temperatures. At low temperatures, the ratio remains relatively flat with system size, while at high temperatures it grows exponentially with system size.

This behavior can be understood by considering the high and low temperature limits of Z_a . We recall that the bath partition function is given by $Z_a = \sum_{\alpha_{i,j}} e^{-\beta\epsilon_{\alpha_{i,j}}}$, where $\epsilon_{\alpha_{i,j}}$ corresponds to the magnitude of the energy difference between system energy eigenvalues E_i and E_j . For an N -site spin chain system the number of eigenvalues is 2^N . In this case, we have $L = 2^N - 1$ while the upper limit of the summation in Z_a will be $\binom{2^N}{2} + 1$. Thus, in the infinite temperature limit we have,

$$\lim_{\beta \rightarrow 0} \frac{Z_a}{L} = \frac{\binom{2^N}{2} + 1}{2^N - 1} = \frac{2^N}{2} + \frac{1}{2^N - 1} \quad (27)$$

Thus, as the system size grows, the ratio Z_a/L , and thus also $g\Delta t$ grow, rendering the approximate expansion for the time evolution operator increasingly inaccurate and leading to the different dynamics between the models observed in Fig. 6.

On the other hand, in the zero temperature limit, the only terms that contribute to Z_a are those where $\epsilon_{\alpha_{i,j}} = 0$. This occurs in the case of the ground state energy of the bath and for any $\epsilon_{\alpha_{i,j}}$ corresponding to degenerate pairs of system energy eigenvalues. As the number of degenerate energy states depends on the system size and model parameters, this leads to the non-monotonic behavior of Z_a/L observed at low temperatures in Fig. 7. In general, as long as the number of pairs of degenerate eigenvalues grows slower than the total number of eigenvalues, the ratio Z_a/L will remain small at low temperatures.

V. CONCLUDING REMARKS

In this work we have verified that both the collisional model framework and the Metropolis algorithm lead to thermalization of a many-body system when, in the case of the collisional model, the spectrum of the bath ancillae corresponds to each of the energy eigenstate transitions in the system. We have then demonstrated analytically that not only do both schemes produce thermalization, but that the time-dependent dynamics generated by both models are exactly equivalent when a condition relating the collisional model interaction strength and the ratio of bath ancilla partition function to number of possible energy eigenstate transitions is fulfilled. We have shown that this condition is more easily fulfilled at small system sizes.

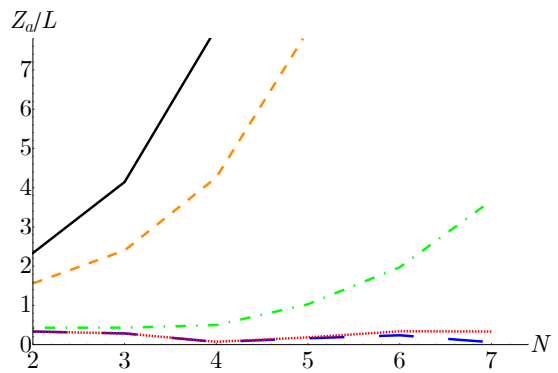


FIG. 7. Ratio of the partition function for the collisional model bath ancillae, Z_a , to the number of possible eigenstate transitions at each time step in the Metropolis algorithm, L , for the one-dimensional XXZ model as a function of chain length N at inverse temperature $\beta = 200$ (blue, long dashed), $\beta = 20$ (red, dotted), $\beta = 2$ (green, dot-dashed), $\beta = 0.2$ (orange, short dashed), and $\beta = 0$ (black, solid). Parameters are $J = h = \Delta = 1$.

Despite the similarities discussed here, there remain some important distinctions between the collisional model and the Metropolis algorithm. By microscopically modeling the system-bath interaction, the collisional model is significantly more general and can be applied with arbitrarily structured bath ancillae to study non-thermal steady states of open system dynamics. Our quantum implementation of the Metropolis scheme also assumes that the system transitions only between individual eigenstates. The collisional model, on the other hand, can model dynamics where the system density matrix has non-zero coherences.

Computationally, the Metropolis algorithm is significantly cheaper as it simply tracks individual eigenstate transitions and needs to know only about the Hilbert space of the system. The collisional model must take into account the much larger joint system-bath Hilbert space and perform repeated partial traces after each system-bath interaction. For example, consider a system whose Hilbert space dimension is d . For modeling thermalizing dynamics using a bath whose spectrum has an excited state corresponding to each transition in the system, as we have done in our demonstration of thermalization in the XXZ model, the Hilbert space of each bath ancilla must be of dimension $\binom{d}{2} + 1$. Thus the total Hilbert space that the collisional model must operate in is of dimension $\mathcal{O}(d^3)$. Even in the most optimal scenario, when the spectra of the bath ancillae are identical to the spectrum of the system, the joint system bath Hilbert space will be of dimension $\mathcal{O}(d^2)$. We must also keep in mind that the Metropolis scheme does incur an additional cost from the fact that the dynamics must be averaged over many repeated runs in order to construct the time-dependent density matrix, while the collisional model directly models the density matrix evolution. However, each Metropolis experimental run still consists of only a

series of products of d -dimensional operators.

These results open several avenues for potential future work. While we have shown an equivalence between the collisional model and Metropolis approaches in thermalizing dynamics, it may be possible to generalize it to generic open system dynamics by modifying the distribution that the accept/reject probabilities are drawn in the Monte Carlo approach. Collisional models have seen extensive use in studying non-Markovian open system dynamics. It would be interesting to see if a similar equivalence could be found between non-Markovian collisional models and non-Markovian Monte Carlo schemes

for quantum evolution [44–46].

ACKNOWLEDGMENTS

We acknowledge support from AFOSR (FA9550-23-1-0034,FA2386-21-1-4081) and ARO (W911NF2210247). We thank the HPC resources at Virginia Tech, where some of the results in this manuscript are generated.

-
- [1] J. M. Deutsch, Quantum statistical mechanics in a closed system, *Phys. Rev. A* **43**, 2046 (1991).
- [2] M. Srednicki, Chaos and quantum thermalization, *Phys. Rev. E* **50**, 888 (1994).
- [3] M. Rigol, V. Dunjko, and M. Olshanii, Thermalization and its mechanism for generic isolated quantum systems, *Nature* **452**, 854 (2008).
- [4] J. Eisert, M. Friesdorf, and C. Gogolin, Quantum many-body systems out of equilibrium, *Nat. Phys.* **11**, 124 (2015).
- [5] R. Nandkishore and D. A. Huse, Many-body localization and thermalization in quantum statistical mechanics, *Annu. Rev. Condens. Matter Phys.* **6**, 15 (2015).
- [6] E. Altman, Many-body localization and quantum thermalization, *Nat. Phys.* **14**, 979 (2018).
- [7] H.-P. Breuer and F. Petruccione, *The Theory of Open Quantum Systems* (Oxford University Press, 2007).
- [8] F. Ciccarello, S. Lorenzo, V. Giovannetti, and G. M. Palma, Quantum collision models: Open system dynamics from repeated interactions, *Phys. Rep.* **954**, 1 (2022).
- [9] N. K. Bernardes, A. R. R. Carvalho, C. H. Monken, and M. F. Santos, Environmental correlations and Markovian to non-Markovian transitions in collisional models, *Phys. Rev. A* **90**, 032111 (2014).
- [10] N. K. Bernardes, A. Cuevas, A. Orioux, C. H. Monken, P. Mataloni, F. Sciarrino, and M. F. Santos, Experimental observation of weak non-Markovianity, *Sci. Rep.* **5**, 17520 (2015).
- [11] F. Ciccarello, G. M. Palma, and V. Giovannetti, Collision-model-based approach to non-Markovian quantum dynamics, *Phys. Rev. A* **87**, 040103 (2013).
- [12] R. McCloskey and M. Paternostro, Non-Markovianity and system-environment correlations in a microscopic collision model, *Phys. Rev. A* **89**, 052120 (2014).
- [13] M. Pezzutto, M. Paternostro, and Y. Omar, Implications of non-Markovian quantum dynamics for the Landauer bound, *New J. Phys.* **18**, 123018 (2016).
- [14] S. Kretschmer, K. Luoma, and W. T. Strunz, Collision model for non-Markovian quantum dynamics, *Phys. Rev. A* **94**, 012106 (2016).
- [15] D. Karevski and T. Platini, Quantum nonequilibrium steady states induced by repeated interactions, *Phys. Rev. Lett.* **102**, 207207 (2009).
- [16] F. Barra, The thermodynamic cost of driving quantum systems by their boundaries, *Sci. Rep.* **5**, 14873 (2015).
- [17] P. Strasberg, G. Schaller, T. Brandes, and M. Esposito, Quantum and information thermodynamics: A unifying framework based on repeated interactions, *Phys. Rev. X* **7**, 021003 (2017).
- [18] S. Seah, S. Nimmrichter, and V. Scarani, Nonequilibrium dynamics with finite-time repeated interactions, *Phys. Rev. E* **99**, 042103 (2019).
- [19] M. Ziman, P. Štelmachovič, and V. Bužek, Description of quantum dynamics of open systems based on collision-like models, *Open Syst. Inf. Dyn.* **12**, 81 (2005).
- [20] F. Ciccarello, Collision models in quantum optics, *Quantum Meas. Quantum Metrol.* **4**, 53 (2017).
- [21] M. Cattaneo, G. De Chiara, S. Maniscalco, R. Zambrini, and G. L. Giorgi, Collision models can efficiently simulate any multipartite Markovian quantum dynamics, *Phys. Rev. Lett.* **126**, 130403 (2021).
- [22] B. M. Terhal and D. P. DiVincenzo, Problem of equilibration and the computation of correlation functions on a quantum computer, *Phys. Rev. A* **61**, 022301 (2000).
- [23] V. Scarani, M. Ziman, P. Štelmachovič, N. Gisin, and V. Bužek, Thermalizing quantum machines: Dissipation and entanglement, *Phys. Rev. Lett.* **88**, 097905 (2002).
- [24] F. Barra and C. Lledó, Stochastic thermodynamics of quantum maps with and without equilibrium, *Phys. Rev. E* **96**, 052114 (2017).
- [25] O. Arisoy, S. Campbell, and O. E. Mustecaphoglu, Thermalization of finite many-body systems by a collision model, *Entropy* **21**, 1182 (2019).
- [26] S. L. Jacob, M. Esposito, J. M. Parrondo, and F. Barra, Thermalization induced by quantum scattering, *PRX Quantum* **2**, 020312 (2021).
- [27] J. Tabanera-Bravo, J. M. R. Parrondo, M. Esposito, and F. Barra, Thermalization and dephasing in collisional reservoirs, *Phys. Rev. Lett.* **130**, 200402 (2023).
- [28] D. P. Landau and K. Binder, *A Guide to Monte Carlo Simulations in Statistical Physics*, 4th ed. (Cambridge University Press, 2014).
- [29] J.-C. Walter and G. Barkema, An introduction to Monte Carlo methods, *Phys. A: Stat. Mech. Appl.* **418**, 78 (2015).
- [30] A. W. Sandvik, Computational studies of quantum spin systems, *AIP Conf.* **1297**, 135 (2010).
- [31] D. M. Ceperley, Metropolis methods for quantum Monte Carlo simulations, *AIP Conf.* **690**, 85 (2003).
- [32] R. J. Glauber, Time-dependent statistics of the Ising model, *J. Math. Phys.* **4**, 294 (2004).
- [33] R. Augusiak, F. M. Cucchietti, F. Haake, and M. Lewen-

- stein, Quantum kinetic ising models, *New J. Phys.* **12**, 025021 (2010).
- [34] S. Andréys, Repeated interaction processes in the continuous-time limit, applied to quadratic fermionic systems, *Ann. Henri Poincaré* **21**, 115 (2020).
- [35] S. N. Filippov and I. A. Luchnikov, Collisional open quantum dynamics with a generally correlated environment: Exact solvability in tensor networks, *Phys. Rev. A* **105**, 062410 (2022).
- [36] N. Metropolis, A. W. Rosenbluth, M. N. Rosenbluth, A. H. Teller, and E. Teller, Equation of state calculations by fast computing machines, *J. Chem. Phys.* **21**, 1087 (1953).
- [37] J. Dalibard, Y. Castin, and K. Mølmer, Wave-function approach to dissipative processes in quantum optics, *Phys. Rev. Lett.* **68**, 580 (1992).
- [38] K. Mølmer, Y. Castin, and J. Dalibard, Monte Carlo wave-function method in quantum optics, *J. Opt. Soc. Am. B* **10**, 524 (1993).
- [39] M. B. Plenio and P. L. Knight, The quantum-jump approach to dissipative dynamics in quantum optics, *Rev. Mod. Phys.* **70**, 101 (1998).
- [40] A. J. Daley, Quantum trajectories and open many-body quantum systems, *Adv. Phys.* **63**, 77 (2014).
- [41] K. Temme, T. J. Osborne, K. G. Vollbrecht, D. Poulin, and F. Verstraete, Quantum Metropolis sampling, *Nature* **471**, 87 (2011).
- [42] U. Wolff, Collective monte carlo updating for spin systems, *Phys. Rev. Lett.* **62**, 361 (1989).
- [43] M. Troyer, F. Alet, S. Trebst, and S. Wessel, Non-local updates for quantum Monte Carlo simulations, *AIP Conf.* **690**, 156 (2003).
- [44] H.-P. Breuer, B. Kappler, and F. Petruccione, Stochastic wave-function method for non-Markovian quantum master equations, *Phys. Rev. A* **59**, 1633 (1999).
- [45] S. Maniscalco, J. Piilo, F. Intravaia, F. Petruccione, and A. Messina, Lindblad- and non-Lindblad-type dynamics of a quantum Brownian particle, *Phys. Rev. A* **70**, 032113 (2004).
- [46] J. Piilo, S. Maniscalco, A. Messina, and F. Petruccione, Scaling of non-Markovian Monte Carlo wave-function methods, *Phys. Rev. E* **71**, 056701 (2005).